Environ Earth Sci (2012) 65:1895–1907
DOI 10.1007/s12665-011-1171-0

ORIGINAL ARTICLE

Multi-risk interpretation of natural hazards for settlements of the Hatay province in the east Mediterranean region, Turkey using SRTM DEM

A. C. Demirkesen

Received: 7 October 2009 / Accepted: 25 June 2011 / Published online: 9 July 2011
© Springer-Verlag 2011

Abstract Many scientists have recently alarmed natural hazards due to global climate change. Such natural disasters are coastal inundation in response to sea-level rise, and/or river flooding caused by heavy rain falls, additionally earthquakes and, etc. In terms of natural hazards, one of the most sensitive and culturally significant areas in Turkey is the Hatay province in the east Mediterranean region. The Hatay province is located on such a region which is not only vulnerable to coastal inundation and river flooding, but also is a tectonically and seismically sensitive area. In this study, for taking conservation measures against the natural hazards beforehand and decision-making on any future land-planning; a digital terrain model and a 3D fly-through model of the Hatay province were generated; then quantitatively and/or qualitatively interpreted by employing the Shuttle Radar Topographic Mission digital elevation model. Besides, stream drainage patterns, lineaments and structural–geological features were extracted for natural hazard risk interpretation of settlements and their relationships among the landscape characteristics were exhibited by combining tectonic information previously confirmed. Regarding the sea-level rise, the coastal inundation risk map indicates that the most vulnerable areas are: coastlines of Iskenderun, Arsuz, Payas and Samandag, respectively. By/after analyzing the digital terrain of the study region and stream drainage patterns, the Karasu Valley Zone, where the Amik plain, settlements of Antakya, Iskenderun, Arsuz, Payas and Samandag with their flood plains have the most flooding risk in decreasing order, respectively when a heavy raining occurs. Finally, analysis of tectonics has revealed that Antakya, Iskenderun, Hassa, Kirikhan, Samandag, Payas, Arsuz, Altinozu, Kumlu and Hacipasa regions have the most sensitivity to earthquake disaster in the study region.

Keywords Digital terrain analysis · Structural geology · Natural hazard risk interpretation · Coastal flood risk · River flood risk · Earthquake risk · Hatay-Turkey

A. C. Demirkesen (✉)
Department of City and Regional Planning,
Izmir Institute of Technology, Izmir, Turkey
e-mail: ademirkesen@yahoo.com

Introduction

The Intergovernmental Panel on Climate Change (IPCC) have recently reported a considerable acceleration (increasing speed) of the global mean sea-level rise (MSLR) due to global climate change and the global MSLR has been alarming coastal communities (IPCC 2001). The global mean sea-level has risen at a rate of 1–2 mm year^{-1} during the last century (Church and White 2006). Besides, Yildiz et al. (2003) also reported acceleration in sea-level rise of 8.7 $\pm$ 0.9 mm year^{-1} between 1984 and 2002 as the local MSLR in the Antalya-II mariograph station in the city of Antalya at the Mediterranean coast in Turkey. If this acceleration continues, then some coastal areas will most likely be under water by the year 2200.

Apart from sensitivity to coastal inundation of the study region, one of the regions under the river flooding risk in response to heavy rain falls is the Hatay province, which is historically and anthropologically one of distinct places in Turkey. Besides, the Hatay province is also tectonically and seismically one of the most sensitive coastal ecosystem areas, as well. The Hatay region is covered with erosion-induced mountain ranges, volcanic sedimentary and tectonic rock structures as well as fertile agricultural soils of plains. Moreover, the Amanos mountains, as a part of this region, is a natural preservation area covered with mostly forest including rich species of fauna and flora. The effects of sea-level rise, such as coastal inundation and erosion are of great economic and ecological significance considering negative changes in this coastal ecosystem.

Advances in the surveying techniques of remote sensing (RS) and tide gauge, and the spatial analysis by geographic information systems (GIS) have provided more accurate data and data processes for the risk interpretation of settlements. Employing RS techniques integrated with GIS, we not only analyzed both the digital terrain model (DTM) and the 3D fly-through model of the study region in terms of interpreting the landscape characteristics; but also extracted and analyzed lineaments indicating faults and/or fractures and/or depressions (collapses) together with the stream drainage patterns and landform structures. Moreover, mapping of naturally sensitive and culturally significant areas constitutes a basis for land use planning and decision-making on preservation and management of natural resources in the environment.

Therefore, objectives of this study were: (1) firstly to acquire geo-information about the study region by quantifying geo-structures (landforms) based on DEM data; (2) secondly to determine spatial distributions of the settlements having the possible natural hazard risks of the coastal inundation and the river flooding as well as the earthquake-sensitive settlements of the study region by employing not only the land-use land-cover (LULC) types obtained from several data sources as GIS layers, but also the DEM obtained by the SRTM; and (3) finally to contribute to decision-making on any future planning of the environment and preservation of the settlements and natural resources.

Materials and methods

Study area

The study area, the province of Hatay, is surrounded by the provinces of Adana at the northwest, Osmaniye at the north, and Gaziantep at the northeast. The eastern and southern sides of the study region have the neighbor country, Syria. The western side is the Mediterranean sea. The Hatay province is located at 35°52′N–37°04′N parallels and 35°40′E–36°35′E meridians. The Hatay province has an area of 5,403 km^2, with ranging elevations of 0–2,240 m and a total population size of about 1.5 million people (Fig. 1). The study region has a Mediterranean climate, with a mild winter and mean annual precipitation of about 1,100 mm and a hot dry summer. Average temperature is of 5°C in January, and 44°C in July (Hatay Governorship 2007).

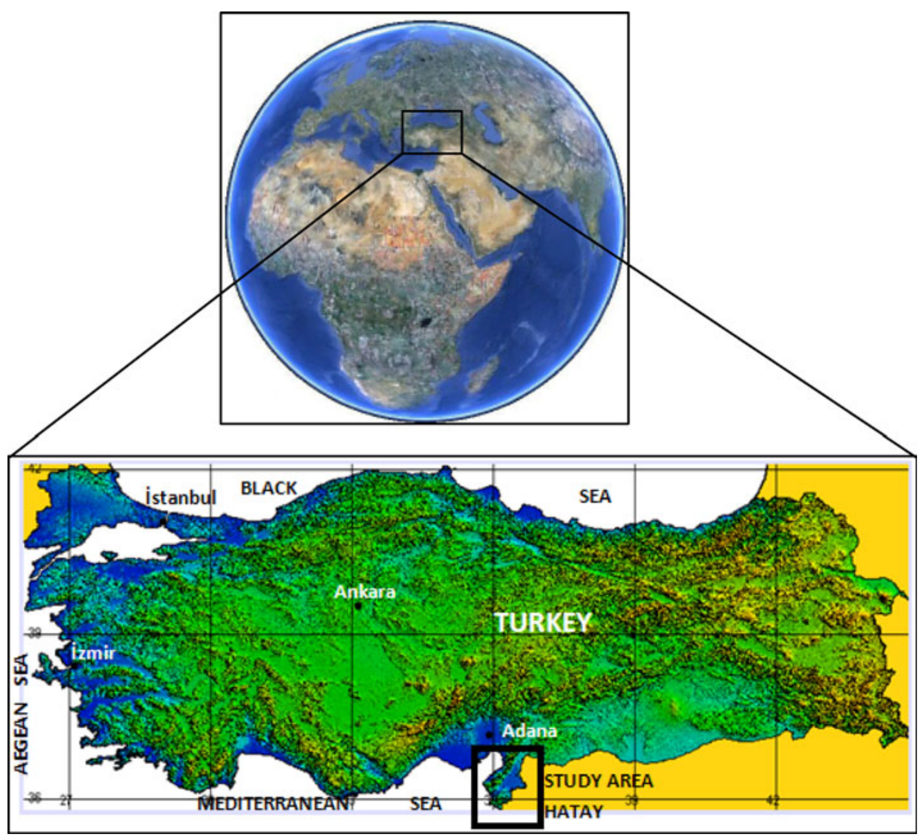

Fig. 1 Location of the study area, the Hatay province in Turkey

Table 1 The landscape characteristics of the study region compiled from the previous studies

Main settlements	Rivers and lakes	Main valleys	River flood plains	Land covers	Fault zones	Mounts (m)
Antakya	Orontes R. (Big Asi R.)	Karasu	Amik plain	1% of settlement	Karasu (Amanos)	Migirtepe (Boz Dag) (2,240) on Amanos
Altinozu	Karasu R.		Orontes	0.5% of water body	East Anatolian	Kuscutepe (2,076) on Amanos
Belen	Afrin R.		Karasu	45% of agriculture	Dead Sea	Kizil Dag (1,750) on Amanos
Dortyol	Small Asi R.		Afrin	20% of plateau	East Hatay	Susuztepe (1,702) on Amanos
Erzin (Yesilkent)	Yarseli Lake			35% of mountain	Reyhanli	Ikiztepe (1,698) on Amanos
Hassa	Beyaz Creek			20% of forest	Afrin	Karliktepe (1,382) on Amanos
Iskenderun	Delicay Creek			13% of bareground and pasture		Musa Dag (1,281)
Kirikhan	Dortyol Creek					Akra Dag (1,729)
Kumlu	Arsuz Creek					Ziyaret Dag (1,235)
Reyhanli	Mersin Creek					Habibneccar Dag (500)
Samandag	Burnaz Creek					
Yayladag	Baglama Lake					
Arsuz (Ulucinar)	Golbasi Lake					
Payas (Yakacik)	Yenisehir Lake					
	Yayladag Lake					

Table 1 compiled from the previous studies shows the landscape characteristics of the Hatay province. All plains in the study region are covered with sedimentary alluviums forming fertile agricultural soils. The alluvial soils, Quaternary deposits on the Amik plain, as river flood plains of Orontes, Afrin and Karasu rivers, form the most fertile agricultural fields at the east of the study region. Besides, the west of the Amanos mountains includes a narrow strip of coastal flood plains such as the plains of Erzin (Yesilkent), Dortyol, Payas (Yakacik), Iskenderun and Arsuz (Ulucinar).

In addition, Over et al. (2011), (p. 314), illustrates the soil and subsoil conditions, volcanic, tectonic and bedrock characteristics of the study region in detail via a geological map of the study area. The geological map shows that the Amanos mountains have mostly Cretaceous structures. The Amik plain and the western river flooding plains have Quaternary deposits. Altinozu area has Miocene and Yayladag area has Upper Cretaceous structures.

In the study region, there is only a big river called Orontes (Big Asi) having several sub-tributaries. The Orontes river is formed by merging of three rivers: (1) the Karasu river, (2) the Afrin river and (3) the Small Asi river. The Karasu river runs in the Karasu Valley Zone (KVZ) having sub-tributaries coming from the Amanos mountains; and merges with the Afrin river; then, in the city of Antakya, joins into the Small Asi river coming from Lebanon. So, the Big Asi (Orontes) river forms. The Afrin river comes from Kilis through the country, Syria and runs in the Amik plain; then, in the Arpahan district of Antakya, merges with the Karasu river. Besides, in the study region, there are also a few creeks running from west sides of the Amanos mountains and discharging into the Mediterranean sea.

As for the land cover of the study region, the west of the region is mainly occupied by the Amanos mountains covered with mostly forest. The east of the region is occupied by the Amik plain and river flood plains.

Several scientists particularly studied on the tectonics of the study region (Yurur and Chorowicz 1998; Rojay et al. 2001; Adiyaman and Chorowicz 2002; Yurtmen et al. 2002; Over et al. 2004; Tatar et al. 2004; Westaway 2004; Akyuz et al. 2006; Korkmaz 2009, 2010; Over et al. 2011).

Yurur and Chorowicz 1998; Rojay et al. 2001; Adiyaman and Chorowicz 2002; Yurtmen et al. 2002; Over et al. 2004; Tatar et al. 2004; Westaway 2004; Akyuz et al. 2006; Over et al. 2011 informed that there is a significant fault zone, the Karasu Fault Zone (KFZ), which bounds the western margin of the KVZ in the Hatay province, takes up a part of the left-lateral slip between the African and

Arabian tectonic plates, that are accommodated farther south on the Dead Sea Fault Zone (DSFZ). They also indicated that tectonics and volcanism developed essentially the east of the DSFZ, the strike-slip boundary of the Arabian and African tectonic plates. They mapped tectonics and volcanism of the study region based on radar imagery and digital elevation models (DEMs); and exhibited the elongate volcanoes, volcanic ridges, linear clusters of adjacent volcanic vents, which are rooted on tension of fractures in kilometers of lengths.

Database development

Shuttle Radar Topography Mission (SRTM) DEM data

SRTM DEM data (Sun et al. 2003; Gorokhovich and Voustianiouk 2006; Farr et al. 2007; The Global Land Cover Facility, http://glcfapp.umiacs.umd.edu:8080/esdi/index.jsp; Shuttle Radar Topography Mission, http://srtm.csi.cgiar.org/SELECTION/inputCoord.asp; Shuttle Radar Topography Mission, United States Geological Survey, http://srtm.usgs.gov/) were employed for this study to obtain geo-information about the study region. The SRTM provided the most complete and medium resolution DEM of the earth (Farr et al. 2007). The SRTM DEM data with spatial resolution of 90 m in World Reference System (WRS) tiles and dated 2000 were used to classify DEM of the Hatay province. The SRTM data, version 2 were freely obtained from the web site: Global Land Cover Facility (GLCF), Earth Science Data Interface (ESDI) (The Global Land Cover Facility, http://glcfapp.umiacs.umd.edu:8080/esdi/index.jsp).

The SRTM acquires elevation data on a near-global scale to generate the most complete medium-resolution digital topographic database of the earth. The SRTM consisted of a specially modified radar system that flew onboard the Space Shuttle Endeavor (The Global Land Cover Facility, http://glcfapp.umiacs.umd.edu:8080/esdi/index.jsp).

The GLCF provides the SRTM data at three resolutions: (1) the 1 arc-second DEM (30 m resolution) of the United States; (2) the 3 arc-second DEM (90 m resolution) of the world that was used in this study; and (3) the 30 arc-second SRTM-GTOPO-30 DEM (1 km resolution).

Maps used in this study

Digital topographic maps (quadrangles) of the study region at the scale of 1:250,000 were obtained from the General Command of Mapping (Turkish: Harita Genel Komutanlığı, HGK). This topographic maps include a few number of GIS layers. Such layers are: settlements, rivers, lakes, roads and boundary maps of study region. These GIS layers of the topographic quadrangles were generated by photogrammetric mapping method in the HGK. In addition to these layers, soil and geological maps of the study region at the scale of 1:1,000,000 were obtained from the General Directorate of Mineral Search and Exploration Institute (Turkish: Maden Tetkik ve Arama Enstitüsü, MTA). All the data were used for geological interpretation and geo-information and locating the settlements and overlaying with our resultant maps in a GIS environment.

Data analysis and interpretation

Processing the SRTM DEM data

In this study, a methodology (Fig. 2), processing multi-scaled different map data sources as spatial data (coordinate information) in addition to non-spatial data (attribute information) of the study region, was performed to acquire geo-information about the study region and determine areas under possible multi-risk of natural disasters. Figure 2 shows the procedures and steps used to quantify and analyze the DTM (Wilson and Gallant 2000; El-Sheimy et al. 2005) of the study region in the sense of the multi-risk interpretation, such as the possible risks of the coastal inundation, river flooding and earthquake in a case study in the Hatay province of Turkey.

The SRTM DEM data (Sun et al. 2003; Farr et al. 2007; The Global Land Cover Facility, http://glcfapp.umiacs.umd.edu:8080/esdi/index.jsp; Shuttle Radar Topography Mission, http://srtm.csi.cgiar.org/SELECTION/inputCoord.asp; Shuttle Radar Topography Mission, United States Geological Survey, http://srtm.usgs.gov/) with spatial resolution of 90 m in WRS having geographic co-ordinates—λ, φ degrees, obtained from the Internet (The Global Land Cover Facility, http://glcfapp.umiacs.umd.edu:8080/esdi/index.jsp), were used to classify the DEM of the Hatay province, exhibiting 0–2 m, high-to-medium coastal risk areas in response to sea-level rise, and were used to extract the stream drainage patterns and lineaments in the study region.

Before the classification process, using the "*Projection*" tool in ArcGIS 9.3 (ArcGIS 2008), the DEM data were automatically transformed from the WRS geographic co-ordinates (λ, φ degrees) into the UTM map projection system co-ordinates (x, y m) with the zone number 36N and the Datum WGS84 ellipsoid. After that, using the "*Extract by Mask*" tool of the Extraction Menu in Spatial Analysis Tool Set in ArcGIS 9.3 (ArcGIS 2008), the relevant DEM data were extracted according to the boundary map of the Hatay province. Next, the extracted DEM data were imported to the Idrisi Taiga system for other processing such as the DEM classification to generate Fig. 3. The DEM classification was performed according to the

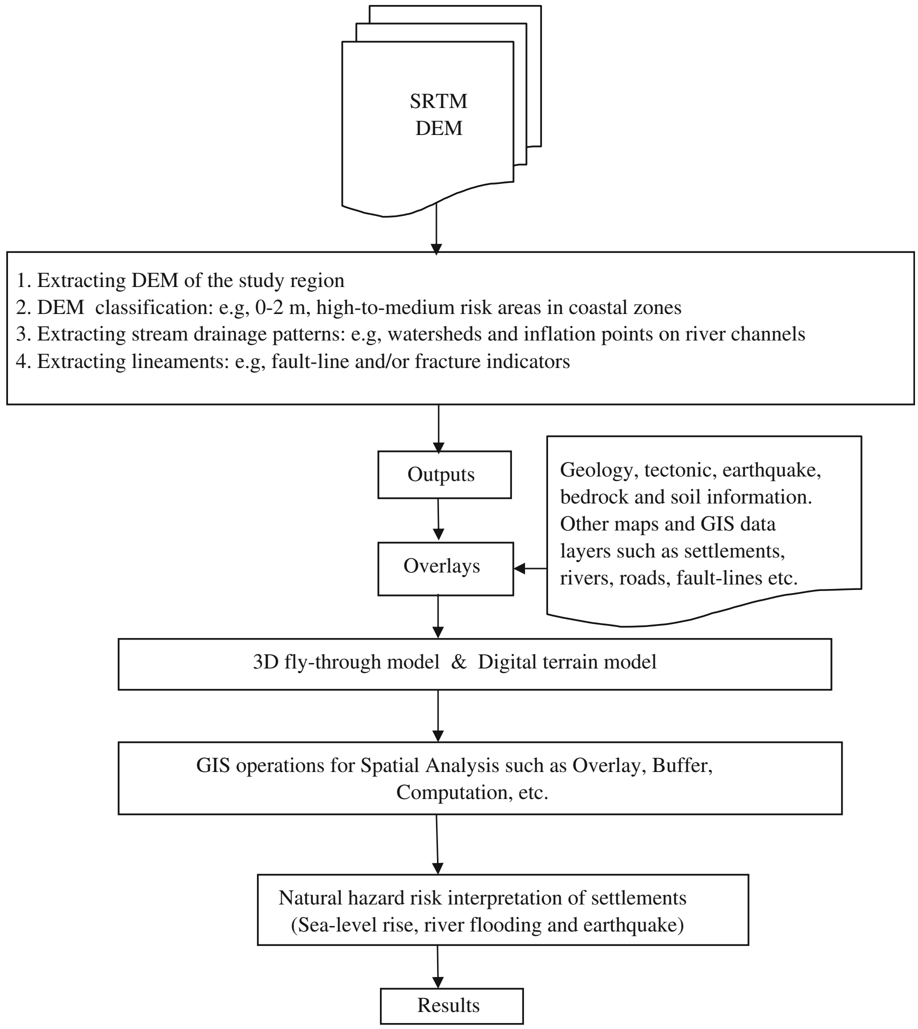

Fig. 2 Methodology: steps of data processes involved in hazard risk interpretation of the settlements of the Hatay province

elevation values of the sudden changes of the land slopes after analyzing the DTM by the tool of "*Display Min/Max Contrast Setting*" in the Idrisi Taiga system. The tool of "*Display Min/Max Contrast Setting*" provides us with monitoring the interactive changes of visualization of the digital terrain according to the elevation values of the terrain. The classified areas in different colors including a number of pixels inside of the grouped class boundaries were computed according to the pixel size of the DEM resolution, 90 m in this case study. This computation procedure was done automatically in the Idrisi Taiga system (Fig. 3; Table 2).

Then, the landform areas such as coastal plains, plateaus and mountain areas in the study region were determined using the SRTM DEM data classification. Next, the landform areas and coastal inundation risky areas in response to projected sea-level rise were computed and analyzed (Fig. 3; Table 2) using the "*GIS Analysis*" Tool Set in a remote sensing environment integrated with a GIS system, the Idrisi Taiga system (Eastman 2003; Idrisi 2009; Demirkesen et al. 2007, 2008).

All the raster cells with the elevations: (1) from 0 to 2 m were designated as high-to-medium risk areas; (2) 2 to 5 m low risk areas; (3) 5 to 25 m coastal plain I; (4) 25 to 250 m coastal plain II; (5) 250 to 500 m lowland; (6) 500 to 1,000 m upland; and (7) 1,000 to 2,240 m mountain after interactively analyzing the digital terrain by the tool of "*Display Min/Max Contrast Setting*" in the Idrisi Taiga system.

Soil and geological maps at the scale of 1:1,000,000 obtained from the General Directorate of Mineral Search and Exploration Institute and the digital topographic maps (quadrangles) at the scale of 1:250,000 of the study area obtained from the General Command of Mapping were used for geological interpretation and geo-information of the study region, as well as for locating the settlements.

Extracting the stream drainage patterns and the lineaments

Many scientists interested in morphology have also studied on the stream drainage patterns and basins as well as coastal zones; and exhibited their relationships among

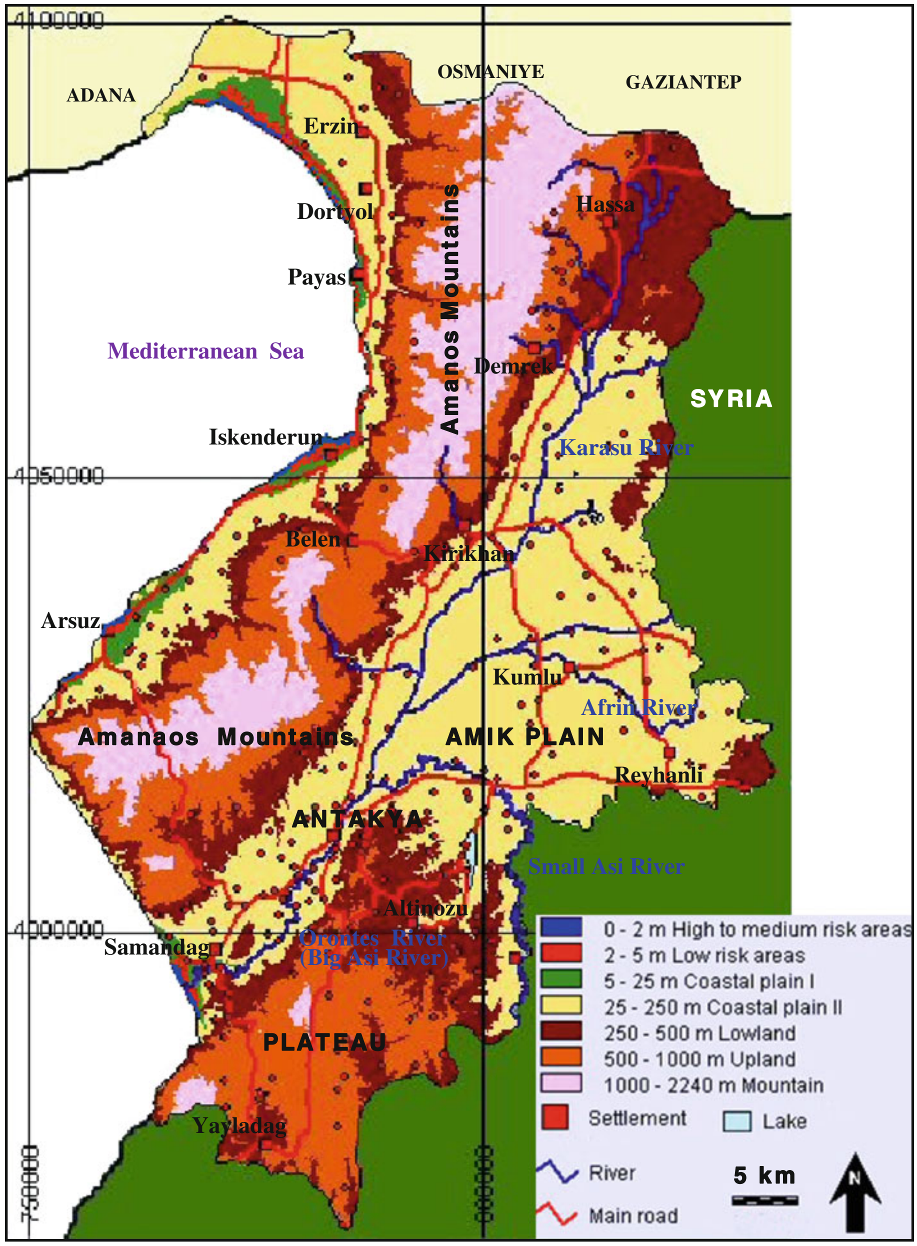

Fig. 3 The risk map showing the coastal inundation and the river flooding risk areas of the Hatay province. Where the areas with the elevations of 0–2 m have the coastal inundation risk and the areas with the elevations of 0–250 m have the river flooding risk

Table 2 The result of the SRTM DEM classification of the Hatay province

Elevation classification	Area (km^2)	Total (%)	Dominant land cover types, respectively
0–2 m high-to-medium risk areas	5	0.1	Bareground/settlement/agriculture
2–5 m low risk areas	25	0.5	Bareground/settlement/agriculture
5–25 m coastal plain I	135	2.5	Agriculture/settlement/waterbody
25–250 m coastal plain II	2,250	41.6	Agriculture/settlement/waterbody
250–500 m lowland	1,115	20.6	Agriculture/settlement/waterbody
500–1,000 m upland	1,183	21.9	Forest/agriculture/settlement
1,000–2,240 m mountain	690	12.8	Forest/bareground
Total study area	5,403	100.0	

Grid size resolution = 90 m; horizontal accuracy = 45 m; and vertical accuracy = 15 m. The study result indicates that: (1) the settlements with altitudes of 0–2 m are located on coastal inundation risk areas, (2) the settlements with altitudes of 0–250 m are located on river flooding risk areas, (3) all the settlements with altitudes of 0–650 m are located on earthquake risk areas (also see Fig. 3) landscape characteristics and landforms (Ray 1960; Siegal and Gillespie 1980; Mark et al. 1984; Band 1986; O'Callaghan and Mark 1984; Pandey 1987; Argialas and Lyon 1988; Prost 1994; Florinsky 1998; Demirkesen 2001, 2009; Drury 2001; Konecny 2002; Avinash et al. 2011; El-Asmar and Hereher 2011, El-Nahry and Doluschitz 2010; Furlan et al. 2011; Hereher 2011; Liang et al. 2011; Ling et al. 2011; Ozdemir and Bird 2009; Yin et al. 2011; Youssef et al. 2011).

In this study, to analyze the digital terrain, the certain characteristics of the digital terrain were employed. For instance, attributes of the elevation values, which indicate sudden changes of the terrain slopes were used not only for the DEM classification, but also for extraction of the stream drainage patterns and lineaments as well as construction of the 3D fly-through model. The stream drainage patterns and lineaments were used for geo-information derivation. The 3D fly-through model showing an interactive visualization of topography and geomorphology was used for interpretation of landforms and the river flooding.

Shaded DEM also called shaded relief or hill shading was used to characterize the digital terrain to extract geo-information such as lineaments, slopes and aspects. Hill shading is hypothetical illumination of the terrain regarding a specified "*azimuth*", 30° used in this case study. Where 0° shows the east as default. Azimuthal increments are in the direction of the counter clock-wise. "*Altitude*" for the the Sun, 80° was used in this case study. Where 90° of the Sun altitude shows the north as default. Shaded DEM generates a 3D effect that provides a sense of visual relief for cartography and a relative measure of incident light for terrain analysis. The shaded DEM was particularly useful not only for extracting the lineaments indicating faults and/or fractures; but also for analyzing the settlements on the terrain in terms of the possible multi-risk interpretation of natural disasters.

In their studies, Jordan (2003) and Jordan and Schott (2005) have widely explained how to extract the lineaments from the DEM. The lineaments determined in the study region have different dimensions and orientations as well as distributions and relationships among them. Lineaments can be differentiated as straight linear or curvilinear features visible on the shaded DEM and give us information about the geological structures. A linear feature may represent a line-variation in the DEM, such as valley-lines, ridge-lines, break-lines and sudden changes of slopes. Therefore, continuous series of pixels as linear features indicate a lineament having similar elevation values. Lineaments are also sometimes identified by continuity and characteristics of spatial textures, as well.

Therefore, faults are usually related to geomorphologic characteristics of features, such as linear boundaries of different formations of geological units, valley-lines, ridge-lines and break-lines that can be determined by lineaments in DTMs. In this study, for instance, the lineaments indicate mainly the six major fault zones (Figs. 4, 5). The main lineaments were obtained by on-screen digitizing from slope, aspect, shaded DEM, DEM segmentation, contours, curvature, directional derivatives and stream drainage patterns. All the digitized lineaments were combined, overlaid, analyzed, and the meaningful lineaments were selected. They were demonstrated overlaying on the settlements by their length and orientation in Fig. 4. For Figs. 4 and 5, the layer of the stream drainage patterns and the other layer including the fault-line and/or fracture indicators were overlaid on the settlements layer, obtained from HGK, in the Idrisi Taiga system, Remote Sensing and GIS environment. Then, the settlements were analyzed with respect to the topography, geomorphology, stream drainage patterns, lineaments and the major fault zones previously confirmed by the scientists (Yurur and Chorowicz 1998; Rojay et al. 2001; Adiyaman and Chorowicz 2002; Yurtmen et al. 2002; Over et al. 2004; Tatar et al. 2004; Westaway 2004; Akyuz et al. 2006).

As for generating the 3D fly-through model, the SRTM of the study region was shaded in colors keeping the same grid size of 90 m and the same co-ordinate reference system, the UTM map projection co-ordinate system with the zone number 36N and the Datum WGS84 ellipsoid. Then, using the "*Fly-through*" tool in the Idrisi Taiga system (Idrisi Taiga 2009), a 3D fly-through model in Fig. 6 was generated by draping the shaded DEM onto the SRTM DEM. The model obtained is a dynamic model so that we can manipulate it for both interactive visualization and analysis in different vertical and horizontal scales and in varying perspective views; such as viewing the landscape from an airplane. The generated model was used to visually and interactively analyze the settlements in terms of the river flooding risk. For doing this, Idrisi Taiga, which is a Remote Sensing and Image Processing system, and ArcGIS, which is a GIS system, providing us with computing, buffering, overlaying, extracting, measuring, cutting, merging, intersecting, etc., were used.

Interpreting the possible multi-risk of natural hazards for the settlements

Basically, the possible risks of the three natural hazards were quantitatively and/or qualitatively (descriptively) determined as multi-risk interpretation of the settlements in this study. Figure 2 shows the methodology of determining the settlements under the multi-risk of natural disasters in the Hatay province.

The first, the coastal inundation disaster risk in response to sea-level rise was quantitatively determined (Fig. 3). Therefore, the DEM of the study region was classified to

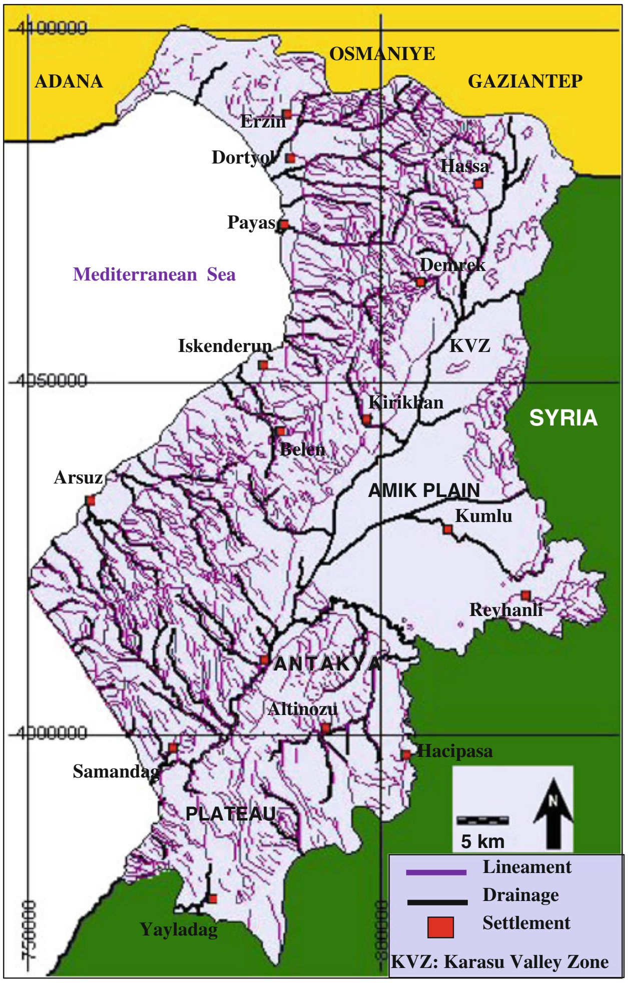

Fig. 4 Lineaments and drainage patterns overlaid with the main settlements in the Hatay province. This map was used for interpretation of the river flooding risk of the main settlements of the Hatay province

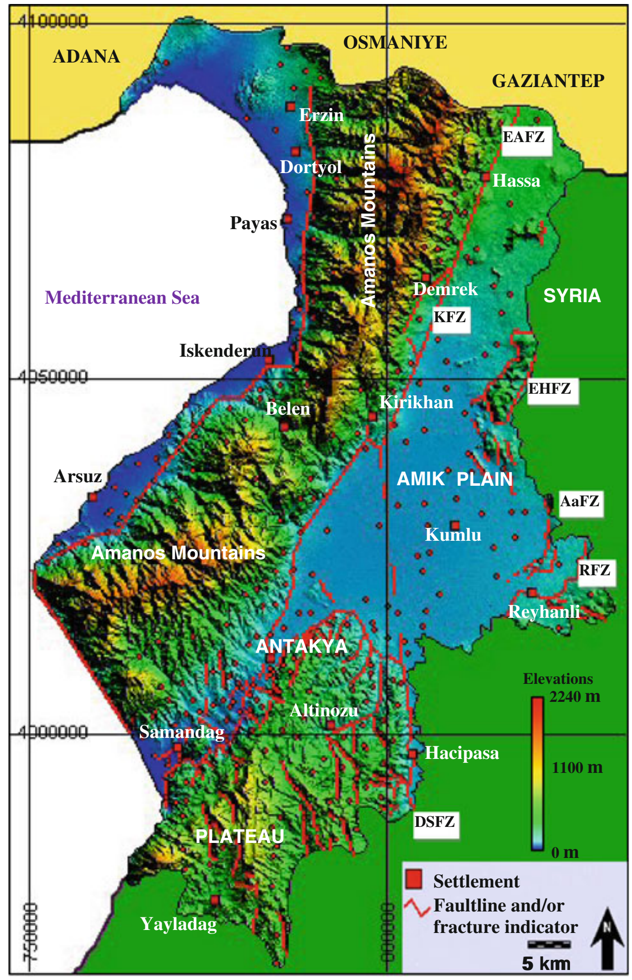

Fig. 5 Fault line and/or fracture indicators overlaid with the settlements in the Hatay province. *EAFZ* East Anatolian Fault Zone, *DSFZ* Dead Sea Fault Zone, *KFZ* Karasu Fault Zone (also called *AFZ* Amanos Fault Zone), *EHFZ* East Hatay Fault Zone, *AaFZ* Afrin Fault Zone, *RFZ* Reyhanli fault Zone

exhibit high-to-medium coastal risk areas (0–2 m) in response to the sea-level rise; in addition to mapping the spatial distribution of the landforms of the study area such as plains, plateaus, mountains and valleys. Figure 3 exhibits the spatial distribution of the settlements with respect to the coastal inundation hazard risk as high-to-medium risk areas in response to sea-level rise. It indicates that the coastlines of Iskenderun, Samandag Arsuz, Erzin, Dortyol and Payas have the coastal flood risk in case of sea-level rise of 2 m or more.

The second, the settlements under the stream flooding risk were interpreted. For this reason, the main stream drainage channels in Strahler order 3 (Demirkesen 2001) and hierarchical watershed drainages (basins or water catchment areas) were automatically captured from the SRTM DEM data using both the "*Hydrology*" tool in ArcGIS 9.3 (ArcGIS 2008) and the "*watershed*" tool of Surface Analysis in Idrisi Taiga system (Demirkesen 2001; Idrisi Taiga 2009). The settlements, located on the main stream drainage channels or on the inflation points (pour points or outlets) or on the main river flood plains, were determined (Figs. 4, 6). Settlements which have flooding risk areas were figured out. In addition, slopes and aspects as well as water flow accumulation areas were extracted to determine the river flood risk areas.

In the river flooding risk interpretation, five criteria were considered to determine risky areas descriptively. (1) Strahler orders of main river channels. (2) Distance of the settlements to the inflation points of the river channels. (3) Distance of the settlements to the river channels. (4) Slopes and aspects of the settlement areas and agricultural plains. (5) Distance of the settlements to the flow accumulation areas. For instance, Antakya is located on such a place where the rivers merge and produce an inflation point on the beginning of the Orontes river in the KVZ. Another example, the Amik plain is rather flat area in terms of

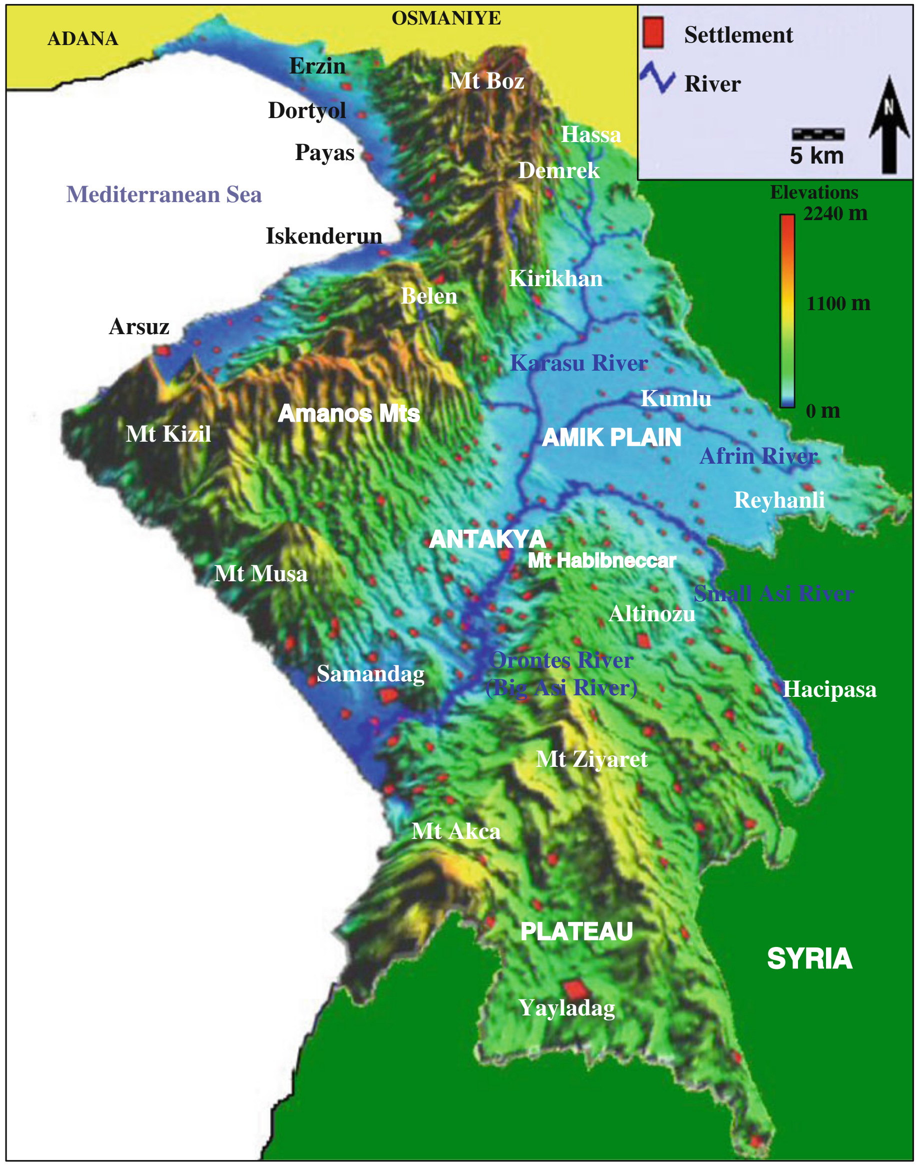

Fig. 6 A perspective view of the 3D fly-through model of the Hatay province. This map was used for interpretation of the river flooding risk of the settlements of the Hatay province, in addition to the digital terrain analysis of the study area

slopes and aspects; as well as, it is a water accumulation area. Also consider that there used to be a lake, called the Amik Lake, in the middle of the Amik plain. The lake was desiccated for the purpose of using the lake area as an agricultural area. But it is now an agricultural area; however, it is under the river flooding risk. Nowadays, settlements are getting increased in these agricultural flood plain areas. Particularly, most water bodies coming from the Amonos mountains not only go through the Antakya city via the Karasu river, but also go through the Amik plain causing an over flooding when heavy rain falls occur. Therefore, the Antakya city and the Amik plain are obviously under the most flood risk. In addition, Fig. 6 shows a 3D fly-through dynamic model, the DTM of the study region in 3D, which can be interactively, qualitatively and visually interpreted in various vertical and horizontal scales in terms of verifying the river flooding risk areas.

The third, the earthquake hazard risk was interpreted. Figure 5 shows an overlay of the settlements with the main fault zones previously confirmed, in addition to the fault-lines and/or fracture indicators and the DTM to analyze the settlements having the earthquake risk. For instance, KFZ is a depression (graben) zone, where the Amonos mountains form a horst and graben as a fault-line zone.

In this risk interpretation, multi-criteria were used for decision-making on determining risky settlements regarding the earthquake hazard, relative to each other. These criteria are: (1) historical background information of the earthquakes occurred in the past and their Richter magnitude scales (M) (Kasapoglu 2007; Korkmaz 2009, 2010;

Tabban 2000). (2) Distance of the settlements to the intersections of the active fault lines. (3) Distance of the settlements to the active fault lines. (4) Ground surface (earth crust) information (rigid-rocky areas or soft-agricultural soils) from the geological maps as terrain factor.

As known, the earthquakes occur on the active fault lines. Intersections of the active fault lines are the most risky locations in terms of the earthquakes. Soft earth crust is more risky than rigid earth crust for the safe constructions. Besides, according to the earthquake map of the country, all over the study region is located on the first degree earthquake region in the country. Thus, all the settlements in the study region are under almost the same earthquake risk of the first degree. However, the four criteria above were used to differentiate slightly the risk levels of the settlements, relative to each other.

For determining the settlements under the earthquake risk; the lineaments indicating faults and/or fractures were extracted and analyzed. Locations of the main fault zones, where the settlements have the possible earthquake risk, were figured out. For instance, Antakya is located on such a place, where the Arabian and Anatolian tectonic plates converge. Antakya also in its history, faced with 7 M of the earthquake in the past as the other settlements faced with about 4–5 M in their historical backgrounds of the earthquake. Thus, Antakya is obviously the most significant under the earthquake catastrophe risk.

For further spatial analysis, after creating the spatial distributions of the settlements, rivers, stream drainage channels, lineaments and fault lines *overlaid* on the digital terrain, some spatial operations such as *Overlay, Buffer, Computation*, etc., were employed (ArcGIS 2008; Avinash et al. 2011; Coppock 1995; Demirkesen 2009; El-Asmar and Hereher 2011; El-Nahry and Doluschitz 2010; Furlan et al. 2011; Hereher 2011; Idrisi Taiga 2009; Liang et al. 2011; Ling et al. 2011; Ozdemir and Bird 2009; Yin et al. 2011; Youssef et al. 2011; Wang et al. 2002). For instance, particularly, "*Buffer*" was used for "range finding" or "finding a certain distance of a settlement to a possible natural hazard risk location". "*Computation*" was used for "computing the areas", consisting of pixel groups in different colors by the GIS environment.

Results and discussion

First of all, based on the analysis of the digital terrain, the results of the DEM classification were: (1) high-to-medium risk areas (total) in response to the projected sea-level rise (0.1%); (2) low risk areas (0.5%); (3) coastal plain I (2.5%); (4) coastal plain II (41.6%); (5) lowland (20.6%); (6) upland (21.9%); (7) mountain (12.8%) of the study region (5,403 km^2) (Fig. 3; Table 2). In sense of coastal inundation vulnerability in response to the projected sea-level rise, the coastal plains (or off shores/coastlines) of Iskenderun, Samandag, Arsuz, Erzin, Dortyol and Payas have most sensitivity to sea-level rise in the study region in decreasing order, respectively (Fig. 3; Table 2).

Secondly, the hierarchical stream drainage patterns in the Strahler order and the lineaments were generated from the SRTM DEM data (Fig. 4); and then analyzed and interpreted in terms of the river flooding risk. Besides, a DTM overlaid with the settlements and the main active fault zones (Fig. 5) and a 3D fly-through dynamic model (Fig. 6) of the study region were generated; and then quantitatively and/or qualitatively interpreted based on the expert opinion in terms of the possible multi-risk of natural hazards.

Analysis of the possible river flooding hazard risk revealed that the main settlements of Antakya, Iskenderun, Arsuz, Payas and Samandag with their river flood plains in addition to the Amik plain have the most risk in the study region, respectively. In other words, most streams come from the Amanos mountains and join into the Orontes river, which runs through the central city of the Antakya and discharges into the Mediterranean sea by making a delta in the coastline of Samandag. Therefore, the most flooding risky areas in the study region are the flood plains of the Orontes river. On the other hand, according to the slopes and aspects, the Amik plain is not only a rather flat plain, but also a water-flow accumulation area. Thus, it is obviously under the river flooding hazard risk significantly when a heavy rain falls.

Thirdly, as known, the faults are usually related to geomorphologic characteristics of features, such as linear boundaries of different formations of geological units, valley-lines, ridge-lines and break-lines that can be determined by lineaments in DTMs. In this study, for instance, the lineaments and the five major fault zones were combined and overlaid on the DTM with the main settlements to generate Fig. 5. Then, it was analyzed and interpreted with regard to the possible earthquake risk. Having analyzed the settlements according to the locations of the major fault lines, the study revealed that Antakya, Hassa, Kirikhan, Samandag, Payas, Iskenderun, Arsuz, Altınozu, Kumlu, Reyhanli and Hacipasa have the most earthquake hazard risk due to the fact that they are located on seismically and tectonically one of the most sensitive and active fault zones. However, Antakya has the most earthquake risk since it is located on intersection of the Arabian and Anatolian tectonic plates which are active.

In summary, interpreting Fig. 3 and Table 2, in general, the study result indicates that: (1) the settlements having mean altitudes of 0–2 m are located on the coastal inundation risk areas; (2) the settlements having mean altitudes of 0–250 m are located on the river flooding risk areas; (3) all the settlements having mean altitudes of 0–650 m are

Table 3 Natural hazard risk interpretation of the main settlements of the Hatay province, relative to each other

Main settlements	Coastal inundation risk level	Flood hazard risk level	Earthquake risk level	Mean altitude of central settlement (m)	Population of central settlement, year 2009
Antakya	No	1	1	85	200,000
Iskenderun	1	2	2	4	320,000
Samandag	3	3	2	10	45,000
Arsuz (Ulucinar)	2	2	2	4	5,000
Dortyol	No	4	3	75	70,000
Payas (Yakacik)	2	2	2	4	35,000
Kumlu	No	4	3	95	15,000
Erzin (Yesilkent)	No	4	3	165	30,000
Kirikhan	No	4	2	150	70,000
Reyhanli	No	4	3	160	60,000
Altinozu	No	No	3	400	10,000
Hassa	No	No	2	400	10,000
Yayladag	No	No	3	450	10,000
Belen	No	No	4	640	20,000

Also, consider that all over the study site is located on the first degree earthquake region in the Country according to the earthquake map of the Country (Kasapoglu 2007; Korkmaz 2009, 2010; Tabban 2000). Thus, all the settlements in the study site are under almost the same earthquake risk of the first degree in the Country

located on the earthquake risk areas. This also means that lower altitudinal areas are in more risk to be coastal inundation and river flooding as well as earthquake in the study region.

On the other hand, according to the Figs. 3, 4, 5 and 6, the study also indicates that the strip zone, consisting of Hassa, Kirikhan, Antakya and Samandag, respectively, which is also called the KVZ or the Amanos Fault Zone (AFZ) are under the most possible risks of both the river flooding and earthquake in the study region. Another strip zone, consisting of the coastlines of Erzin, Dortyol, Payas, Iskenderun and Arsuz, respectively, are under the most possible risk of the coastal inundation and they have also both the river flooding and earthquake risks, as well. Besides, the Amik plain is also under the possible risks of both the river flooding and earthquake.

Having obtained geo-information about the study region employing Figs. 3, 4, 5 and 6 for interpretation of all the settlements under the possible multi-risk of natural hazards, the resultant Tables 2 and 3 were created and they show the possible multi-risk levels of the natural hazards for the main settlements, relative to each other in the Hatay province. The used methodology (Fig. 2) can be efficiently applied on any other coastal regions, such as Istanbul, Izmir and Adana in the Country.

Findings of the study revealed that Antakya with population of 200,000, which is settled in a valley, an active fault zone between the Amanos mountains (average 2,000 m) and Mt Habibneccar (500 m), has the highest risks of the river flooding and the earthquake vulnerability in the study region. In the coastal inundation risk interpretation in response to the projected sea-level rise, the coastlines of Iskenderun is the most risky area with population of 320,000 and with average altitude of 4 m.

For quality assessment of the results, the resolution of the SRTM DEM data was considered for the quality of the methodology used in this study. The SRTM DEM data has the spatial resolution of 90 m with horizontal and vertical accuracies of 45 and 15 m, respectively.

All the results coming from the SRTM DEM data and the other topographic and thematic map data having the different accuracies and scales, revealed the Figs. 3, 4, 5 and 6 and Tables 2 and 3 with these accuracies. And the settlements under the possible multi-risk of natural hazards in the study region were determined and presented after quantitative and/or qualitative analysis as well as descriptive interpretation.

In addition to interpretation of the natural risky areas, quantifying geological structures with their height characteristics in the study region are also quite beneficial and useful for decision-making on important project works in the future. For instance, the locations of tectonic and volcanic structures and stream drainage patterns in the study region are important for decision-making on the selection of suitable sites for houses, hospitals, schools, airports, freeways, railways, dams, etc.

Conclusion

The objective of this study was to obtain geo-information effectively and determine the possible multi-risk of the coastal inundation, river flooding and earthquake in the case study of the Hatay province to contribute to any future planning works, such as protection of the environment during regional planning and conservation of natural resources as well as efficient use of agricultural irrigations, etc.

In this study, in addition to quantifying the landforms such as valleys, plains, plateaus and mountains, a 3D fly-through dynamic model of the Hatay province was generated and interpreted based on the SRTM DEM data. Moreover, to obtain geo-information about the study region, the stream drainage patterns and lineaments were extracted. All of them were used for analyzing and interpreting the DTM of the study region in terms of the possible risk of natural disasters. The study basically indicates that the lower altitudinal areas are under more risk than upper areas in sense of the possible multi-risk of the natural hazards in the study region.

The accuracy of the study depends on the resolution of the grid sizes of the DEM data, processing errors, quality of measurements, registration, transformation and map projection. The methodology would produce more detailed and accurate results if higher resolution DEMs were employed; particularly 5–10 m resolution of grid size. Nevertheless, the results with this data accuracy were quite satisfactory for indicating the settlements which have possible natural hazard risks, relative to each other.

The methodology, quantitatively and/or descriptively interpreting the possible risk of natural disasters in the landscape of the study region can be applied on any other coastal regions in the Country by capturing geo-information from remotely sensed DEM data by an application in a remote sensing environment integrated with GIS, where the data come from both different resolutions and scales.

Acknowledgments Financial support from Izmir Institute of Technology is gratefully acknowledged. The anonymous referees are thanked for their invaluable comments and suggestions on the structure of the manuscript.

References

Adiyaman O, Chorowicz J (2002) Late Cenozoic tectonics and volcanism in the north western corner of the Arabian plate: a consequence of the strike-slip Dead Sea fault zone and the lateral escape of Anatolia. J Volcanol Geotherm Res 117:327–345

Akyuz HS, Altunel E, Karabacak V, Yalciner CC (2006) Historical earthquake activity of the northern part of the Dead Sea Fault Zone, southern Turkey. Tectonophysics 426:281–293

ArcGIS 9.3 Manual (2008) ESRI, New York Street, Redlands, CA. http://www.esri.com/

Argialas DP, Lyon JG (1988) Quantitative description and classification of drainage patterns. Photogramm Eng Remote Sens 54(4):505–509

Avinash K, Jayappa KS, Vethamony P (2011) Evolution of Swarna estuary and its impact on braided islands and estuarine banks, Southwest coast of India. Environ Earth Sci. doi:10.1007/s12665-011-1128-3

Band LE (1986) Topographic partition of watersheds with digital elevation models. Water Resour Res 22(1):l5–l24

Church JA, White NJ (2006) A 20th century acceleration in global sea-level rise. Geophys Res Lett 33:L01602. http://dx.doi.org/10.1029/2005GL024826

Coppock JT (1995) GIS and natural hazard: an overview from a GIS perspective. In: Carrera A, Guzzetti F (eds) Geographical information systems in assessing natural hazards. Kluwer, The Netherlands, pp 21–34

Demirkesen AC (2001) Constructing a prior information-base for river mapping from digital images and DEMs by an advanced image interpretation system. PhD Dissertation, The Ohio State University, Columbus, Ohio, USA

Demirkesen AC (2009) Quantifying geological structures of the Nigde province in central Anatolia, Turkey using SRTM DEM data. Environ Geol 56:865–875

Demirkesen AC, Evrendilek F, Berberoglu S, Kilic S (2007) Coastal flood risk analysis using Landsat-7 ETM+ imagery and SRTM DEM: a case study of Izmir, Turkey. Environ Monit Assess 131:293–300

Demirkesen AC, Evrendilek F, Berberoglu S (2008) Quantifying coastal inundation vulnerability of Turkey to sea-level rise. Environ Monit Assess 138:101–106

Drury SA (2001) Image interpretation in geology. Blackwell Science, London

Eastman R (2003) Idrisi Klimanjaro Manual and Tutorial. Clark Labs, Clark University, Worchester

El-Asmar HM, Hereher ME (2011) Change detection of the coastal zone east of the Nile Delta using remote sensing. Environ Earth Sci 62:769–777

El-Nahry AH, Doluschitz R (2010) Climate change and its impacts on the coastal zone of the Nile Delta, Egypt. Environ Earth Sci 59:1497–1506

El-Sheimy N, Valeo C, Habib A (2005) Digital terrain modeling: acquisition, manipulation and applications. Artech House, Boston

Farr TG, Rosen PA, Caro E, Crippen R, Duren R, Hensley S, Kobrick M, Paller M, Rodriguez E, Roth L, Seal D, Shaffer S, Shimada J, Umland J, Werner M, Oskin M, Burbank D, Alsdorf D (2007) The Shuttle Radar Topography Mission. Rev Geophys 45:RG2004. doi:10.1029/2005RG000183

Florinsky IV (1998) Combined analysis of digital terrain models and remotely sensed data in landscape investigations. Prog Phys Geogr 22(1):33–60

Furlan A, Bonotto DM, Gumiere SJ (2011) Development of environmental and natural vulnerability maps for Brazilian coastal at Sao Sebastiao in Sao Paulo State. Environ Earth Sci. doi:10.1007/s12665-010-0886-7

Gorokhovich Y, Voustianiouk A (2006) Accuracy assessment of the processed SRTM-based elevation data by CGIAR using field data from USA and Thailand and its relation to the terrain characteristics. Remote Sens Environ 104:409–415

Hatay Governorship (2007) Hatay, Turkey. http://www.hatay.gov.tr/

Hereher ME (2011) Mapping coastal erosion at the Nile Delta western promontory using Landsat imagery. Environ Earth Sci. doi:10.1007/s12665-011-0928-9

Idrisi Taiga 16.0 Manual (2009) Clark labs, Clark University Worcester, MA. http://www.clarklabs.org/

IPCC (2001) Climate change 2001: impacts, adaptation, and vulnerability. In: McCarthy JJ, Canziani OF, Leary NA, Dokken DJ, White KS (eds) Contribution of Working Group II to the Third Assessment Report of the Intergovernmental Panel on Climate Change (IPCC). Cambridge University Press, Cambridge

Jordan G (2003) Morphologic analysis and tectonic interpretation of digital terrain data: a case study. Earth Surf Process Landf 28:807–822

Jordan G, Schott B (2005) Application of wavelet analysis to the study of spatial pattern of morphotectonic lineaments in digital terrain models. A case study. Remote Sens Environ 94:31–38

Kasapoglu KE (2007) Things that we want to know about earthquakes and Turkey. The Chamber of Geology Engineering, publishing no: 9, Ankara (in Turkish)

Konecny G (2002) Geoinformation: remote sensing, photogrammetry and geographical information systems. Taylor and Francis, London

Korkmaz KA (2009) Earthquake disaster risk assessment and evaluation for Turkey. Environ Geol 57:307–320

Korkmaz KA (2010) Integrated seismic hazard evaluation and disaster management approach for Turkey. Environ Earth Sci 61:467–476

Liang W, Yongli C, Hongquan C, Daler D, Jingmin Z, Juan Y (2011) Flood disaster in Taihu Basin, China: causal chain and policy option analyses. Environ Earth Sci 63:1119–1124

Ling H, Xu H, Shi W, Zhang Q (2011) Regional climate change and its effects on the runoff of Manas River, Xinjiang, China. Environ Earth Sci. doi:10.1007/s12665-011-1048-2

Mark DM, Dozier J, Frew J (1984) Automated basin delineation from digital elevation data. Geo-Processing 2:299–311

O'Callaghan JF, Mark DM (1984) The extraction of drainage networks from digital elevation data. Comput Vis Graph Image Process 28:328–344

Over S, Ozden S, Yilmaz H (2004) Late Cenozoic stress evolution along the Karasu valley, SE, Turkey. Tectonophysics 380:43–68

Over S, Buyuksarac A, Bekta O, Filazi A (2011) Assessment of potential hazard and site effect in Antakya (Hatay Province), SE Turkey. Environ Earth Sci 62:313–326

Ozdemir H, Bird D (2009) Evaluation of morphometric parameters of drainage networks derived from topographic maps and DEM in point of floods. Environ Geol 56:1405–1415

Pandey SN (1987) Principles and applications of photo geology. John Wiley and Sons, New York

Prost GL (1994) Remote sensing for geologists: a guide to image interpretation. Taylor and Francis Inc., London

Ray RG (1960) Aerial photographs in geologic interpretation and mapping. United States Geological Survey, Washington

Rojay B, Heinmannn A, Toprak V (2001) Neotectonic and volcanic characteristics of the Karasu fault zone (Anatolia, Turkey): the transition zone between the Dead Sea transform and the East Anatolian fault zone. Geodinamica Acta 14:197–212

Siegal BS, Gillespie AR (1980) Remote sensing in geology. John Wiley and Sons, New York

Sun G, Ranson KJ, Kharuk VI, Kovacs K (2003) Validation of surface height from shuttle radar topography mission using shuttle laser altimeter. Remote Sens Environ 88:401–411

Tabban A (2000) Geology of cities and earthquake condition. The Chamber of Geology Engineering, publishing no: 56, Ankara (in Turkish)

Tatar O, Piper JDA, Gursoy H, Heiman A, Kocbulut F (2004) Neotectonic deformation in the transition zone between the Dead Sea Transform and the East Anatolian Fault Zone, Southern Turkey: a palaeomagnetic study of the Karasu Rift Volcanism. Tectonophysics 385:17–43

Wang Y, Colby JD, Mulcahy KA (2002) An efficient method for mapping flood extent in a coastal flood plain using Landsat TM and DEM data. Int J Remote Sens 23:3681–3696

Westaway R (2004) Kinematic consistency between the Dead Sea Fault Zone and the Neogene and Quaternary left-lateral faulting in SE Turkey. Tectonophysics 391:2003–2237

Wilson JP, Gallant JC (2000) Terrain analysis: principles and applications. John Wiley and Sons, New York

Yildiz H, Demir C, Gurdal MA, Akabali OA, Demirkol OE, Ayhan ME et al (2003) Analysis of sea level and geodetic measurements of Antalya-II, Bodrum-II, Erdek and Mentes tide gauges in the period of 1984–2002. J Mapp 17:1–75 (in Turkish)

Yin J, Yin Z, Hu X, Xu S, Wang J, Li Z, Zhong H, Gan F (2011) Multiple scenario analyses forecasting the confounding impacts of sea level rise and tides from storm induced coastal flooding in the city of Shanghai, China. Environ Earth Sci 63:407–414

Youssef AM, Pradhan B, Hassan AM (2011) Flash flood risk estimation along the St. Katherine road, southern Sinai, Egypt using GIS based morphometry and satellite imagery. Environ Earth Sci 62:611–623

Yurtmen S, Guillou H, Westaway R, Rowbotham G, Tatar O (2002) Rate of strike-slip motion on the Amanos Fault (Karasu Valley, southern Turkey) constrained by K–Ar dating and geochemical analysis of Quaternary basalts. Tectonophysics 344:207–246

Yurur MT, Chorowicz J (1998) Recent volcanism, tectonics and plate kinematics near the junction of the African, Arabian and Anatolian plates in the eastern Mediterranean. J Volcanol Geotherm Res 85:1–15